J Solid State Electrochem (2012) 16:803–809
DOI 10.1007/s10008-011-1432-6

ORIGINAL PAPER

Facile preparation of Sb and oxide-coated Sb nanoparticles via cathodic dispersion of bulk Sb in different media

Yingchang Yang · Wei Huang · Jufang Zheng · Zelin Li

Received: 13 February 2011 / Revised: 4 May 2011 / Accepted: 5 May 2011 / Published online: 20 May 2011
© Springer-Verlag 2011

Abstract We report here a facile electrochemical method on the preparation of antimony nanoparticles (NPs) by dispersing a bulk antimony electrode under highly cathodic polarization in different media at room temperature, requiring neither precursor ions nor organic capping agents. The dispersion of bulk antimony in a tetrabutyl ammonium bromide (TBAB) acetonitrile solution involved the formation and oxidation of an unstable Zintl compound of antimony, and the as-prepared Sb NPs were readily transferred into Sb–Sb_2O_3 core–shell NPs during the post treatment and characterization because of the surface oxidation of Sb NPs by oxygen in the air. In contrast, Sb NPs prepared by dispersing the bulk antimony cathode in a blank aqueous NaOH solution were oxygen-resistant in the air because the strongly adsorbed hydroxide ions from the solution could stabilize the Sb NPs. The incorporation of sodium, the formation/oxidation of polyanions of antimony (Zintl ions), and the formation/decomposition of unstable antimony hydrides may all take effect for the cathodic dispersion of bulk antimony electrodes in the NaOH solution. Transmission electron microscope, X-ray diffraction, X-ray photoelectron spectroscopy and Raman spectroscopy were used to characterize these NPs.

Y. Yang · W. Huang · Z. Li (✉)
Key Laboratory of Chemical Biology and Traditional Chinese Medicine Research (Ministry of Education of China),
College of Chemistry and Chemical Engineering,
Hunan Normal University,
Changsha 410081, China
e-mail: lizelin@hunnu.edu.cn

J. Zheng
Key Laboratory of the Ministry of Education for Advanced Catalysis Materials, Institute of Physical Chemistry,
Zhejiang Normal University,
Jinhua 321004, China

Keywords Antimony · Nanoparticles · Cathodic dispersion · Zintl ions

Introduction

Antimony and antimony-based nanomaterials have been attracting wide attention due to their broad applications in such areas as lithium ion batteries [1–3] and electrochemical sensors [4, 5].

Sb nanomaterials have been prepared either by top–down physical methods or by bottom–up chemical methods. The former category includes vapor deposition [6] and spark discharge generation [3]. They involved thermal evaporation of solid antimony and vapor condensation. The latter comprises reduction of $SbCl_3$ by $NaBH_4$ in *N*,*N*-dimethylformamide [7], microwave assisted reduction of antimony sodium tartrate by zinc powder [8], electrodeposition [1, 5], photochemical polythiol processes [9] and thermal decomposition of Sb precursor $Sb(acac)_3$ (acac = acetylacetonate) [2]. To the best of our knowledge, these physical and chemical methods required sophisticated equipments and precursor salts plus organic protective agents, respectively.

Recently, we have developed some facile electrochemical methods synthesizing metal nanomaterials by dispersing bulk metal electrodes. For example, hydrosols of Pt [10] and Rh [11] were prepared with corresponding bulk electrodes in NaOH solutions under potential perturbations of square waves. They involved repeated metal redox and intense hydrogen release. Bi, Sn and Pb nanoparticles (NPs) were prepared via cathodic dispersion of bulk electrodes of Bi [12], Sn and Pb [13], respectively, in aqueous NaOH solutions, involving hydrogen release and formation/decomposition of unstable metal hydrides [14].

In this article, we extended our work to the preparation of Sb NPs by cathodic dispersion of a bulk antimony

electrode, emphasizing the medium effect. The differences in product and in mechanism have been discussed for two different media employed: a tetrabutyl ammonium bromide (TBAB) acetonitrile solution and an aqueous NaOH solution.

Experimental section

Preparation of Sb NPs

Cathodic dispersion experiments were performed with a CHI 660C electrochemical workstation (Chenhua Instruments, Shanghai, China) at room temperature (~25 °C). An antimony wire (2.5 mm in diameter, purity ≥99.9999%) embedded in the epoxy resin mold was used as the working electrode. A Pt sheet (12 mm in length, 10 mm in width) was employed as the counter electrode. A Pt wire (1 mm in diameter) and a saturated mercurous sulfate electrode (SMSE) were chosen as the reference electrode in acetonitrile and in aqueous solution, respectively. Prior to use the Sb electrode was polished with 1200 grit Carbimet paper, and then rinsed with ultrasonic waves in Millipore water. Sb NPs were prepared either in 10 ml of 0.1 M TBAB acetonitrile solution or in 10 ml of 4 M NaOH aqueous solution by cathodic polarization under a given voltage (with two electrodes) or potential (with three electrodes). The catholyte was degassed by Ar gas flow for 15 min to move oxygen before electrolysis. However, no apparent effect was observed with or without purging flow of Ar. The reasons might be (1) the produced hydrogen gas at cathode accompanying the dispersion of Sb electrodes can act as the purging gas during the electrolysis, and (2) the small amount of dissolved oxygen can be easily removed by reduction under the highly cathodic polarization. A modified conventional H-type cell (Fig. 1) with three electrodes and a Luggin capillary was used, where the surface of the working electrode was orientated upwards to facilitate the gas release. The distance between the surface of the working electrode and the Luggin capillary was about 2 mm. Only two electrodes were employed in preparing Sb NPs in acetonitrile for simpleness. The Sb NPs dispersed in acetonitrile and in aqueous NaOH solutions were collected by centrifugation at 12,000 and at 8,000 rev/min, respectively, which were then rinsed by ethanol for six times. The cleaned Sb NPs were centrifugated and dried at room temperature under Ar flow for the tests of X-ray diffraction (XRD), Raman, X-ray photoelectron spectroscopy (XPS) and transmission electron microscopy (TEM).

Characterizations

XRD patterns of Sb NPs were investigated with an X-ray diffractometry (X'Pert PW3040/60, Philips, the Netherlands) equipped with a Philips Analytical X'Celerator, using Cu Kα radiation in a 2θ range from 20° to 70° with a scan rate of $0.2°s^{-1}$. The working voltage of was 40 kV and the current was 40 mA. The samples were loaded on a glass substrate by dropping the suspension of Sb NPs in ethanol and followed by drying at room temperature. The morphology of the prepared Sb NPs loaded on a copper grid by the same operation were characterized by a TEM (FEI model Tecnai F20). The morphologies of Sb electrodes after cathodic dispersion were characterized by a Hitachi S-4800 field emission scanning electron microscope (FESEM). The surface chemical states of the NPs prepared in the NaOH solution were measured by XPS (Kratos Axis Ultra DLD) with an Al Kα X-ray source operated at 120 W with a 15-kV acceleration voltage. Raman spectra of the NPs were measured with a Renishaw1000 model confocal microscopy Raman spectrometer. The excitation laser was 514 nm and a 50× long working-length objective was used.

Results and discussion

Preparation and characterizations of Sb NPs in the TBAB acetonitrile solution

Figure 2A(a) shows the linear scan voltammogram for the bulk Sb cathode in 0.1 M TBAB acetonitrile solution using the three-electrode cell, where the current reached to a steady state while the potential (versus Pt wire) was negative

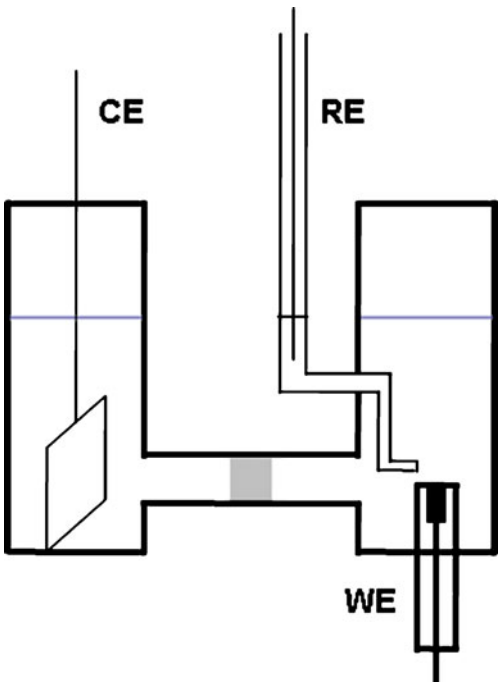

Fig. 1 A schematic cell used for the preparation of Sb NPs, wherein WE, CE and RE represent the working, counter and reference electrode, respectively

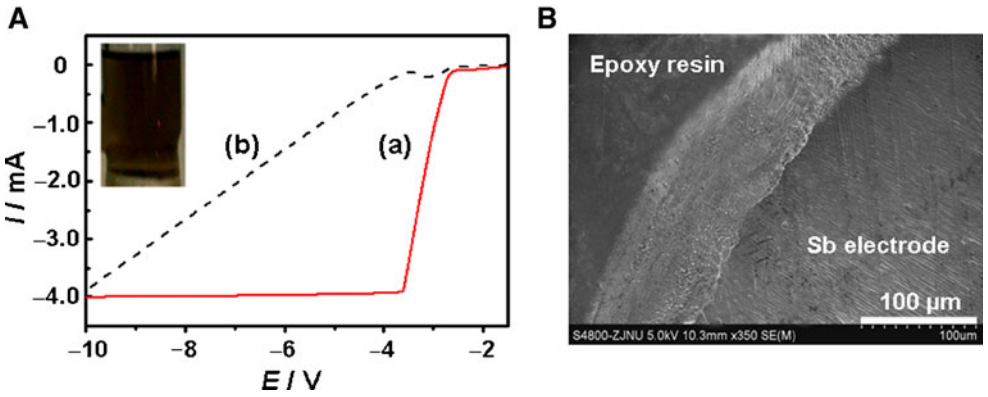

Fig. 2 **A** Linear scan voltammogram at 100 mV/s for the polished bulk Sb electrode (2.5 mm diameter) in 0.1 M TBAB acetonitrile solution with **a** a three-electrode or **b** a two-electrode configuration. *Inset*: Sb colloid from the cathodic dispersion of the Sb electrode in 0.1 M TBAB acetonitrile solution. **B** SEM image of Sb electrode after cathodic dispersion in 0.1 M TBAB acetonitrile solution for 1,000 s

to ca. −3.6 V. In the case of the two-electrode cell, the current increased with the applied voltage and approached to a current at 10 V comparable to the steady current observed in the three-electrode cell. The dispersion of Sb electrode commenced at a voltage of −5 V and a potential of −2.8 V, respectively. To obtain enough Sb NPs quickly in 1,000 s, a voltage of −10 V and a potential of −4 V can be chosen for the configurations of two electrodes and three electrodes, respectively. For simplicity, the two-electrode configuration was adopted here for the preparation of Sb NPs in acetonitrile. During the cathodic polarization process of Sb electrode at −10 V in the 0.1 M TBAB acetonitrile solution, 2 ml of anhydrous ethanol was added drop by drop to the catholyte within one min. Meanwhile, a thin dark yellow stream sprang from the cathode into the solution continuously. But alcohol, addition of methanol, isopropanol, propanol or butanol could also lead to cathodic dispersion. As shown in Fig. 2B, the electrode surface of Sb became rough after cathodic dispersion for 1,000 s in 0.1 M TBAB acetonitrile solution and the Sb wire electrode was ca. 90 μm shorter in length as a result of the dispersion. The metal loss of the Sb electrode was about 3 mg estimated from the lost volume of the electrode and the density of Sb, which should be balanced by the produced Sb colloid (the inset photo in Fig. 2A) in the catholyte since Sb NPs was low reactive with acetonitrile, TBAB and ethanol.

The TEM image in Fig. 3a shows that the average size of Sb NPs prepared in TBAB acetonitrile solution is about 15 nm. It can also be seen that their black cores are surrounded with white coatings of Sb_2O_3. The high-resolution TEM image in Fig. 3b clearly reveals the Sb–Sb_2O_3 core–shell structure of the prepared NPs, where the fringe spacings of 0.309 nm (the core) and 0.324 nm (the shell) can be indexed to those planes of (012) of hexagonal Sb (JCPDS 85–1323) and those planes of (012) of cubic Sb_2O_3 (JCPDS 72–1334), respectively. The Sb_2O_3 coating is about 2 to 3 nm in thickness.

The XRD patterns shown in Fig. 4a for the as-prepared NPs in TBAB acetonitrile solution at room temperature indicate that they were amorphous. Crystallization occurred after being heated to 225 °C for 15 min under Ar atmosphere, which is consistent with previous reports [15–18]. Moreover, Fig. 4b shows that the NPs do contain both hexagonal Sb (JCPDS 85–1323) and cubic Sb_2O_3 (JCPDS 72–1334). Comparing the XRD patterns in Fig. 4 with the high-resolution TEM image in Fig. 3a for the Sb

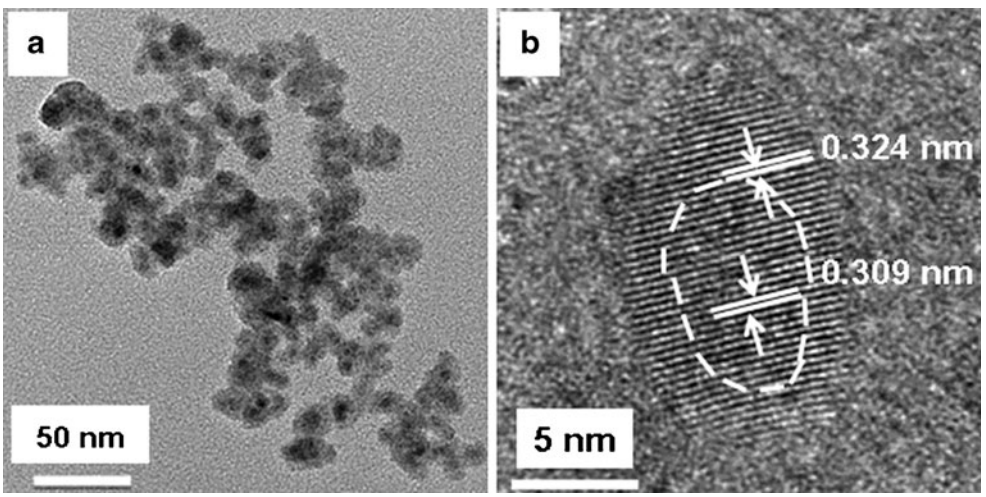

Fig. 3 Typical TEM images of Sb NPs prepared in 0.1 M TBAB acetonitrile solution under **a** lower and **b** higher resolution. The *white dashed line* in (b) roughly indicates the boundary between the Sb core and the Sb_2O_3 shell

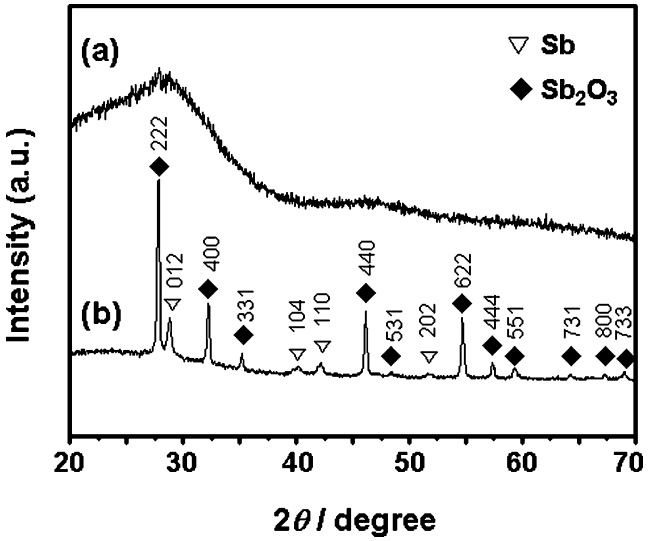

Fig. 4 XRD patterns of Sb NPs prepared in 0.1 M TBAB acetonitrile solution **a** before and (b) after heating to 225 °C for 15 min under Ar atmosphere

NPs, we speculate that the strong TEM beam could engender the crystallization of the amorphous Sb NPs. No such re-crystallization occurred spontaneously by keeping the amorphous Sb NPs at room temperature for a long period of time, say 15 days.

The Sb–Sb_2O_3 core–shell structure of the NPs was further confirmed by Raman spectroscopy. Figure 5a shows the Raman spectrum of freshly prepared Sb NPs in the TBAB acetonitrile solution. The two peaks at 113 and 147 cm^{-1} are characteristic for antimony [1, 19, 20] and the three relatively weak peaks at 190, 252 and 451 cm^{-1} are characteristic for Sb_2O_3 [1, 21]. Figure 5b shows the Raman spectrum recorded for the Sb NPs which were heated to 225 °C for 15 min under Ar atmosphere, where the peaks at 118, 190, 251, 371 and 449 cm^{-1} for Sb_2O_3 became stronger. These facts indicate that the Sb NPs prepared in the TBAB acetonitrile solution could be easily oxidized by oxygen in the air during post treatment and characterization, forming metal-oxide core–shell NPs.

Preparation and characterizations of Sb NPs in the NaOH solution

Figure 6a shows the linear scan voltammogram for the bulk Sb electrode in 4 M NaOH with the three-electrode cell. As the potential (versus SMSE) went negatively to ca. −4.3 V, the current reached to a nearly steady state. We observed that dark black Sb hydrosols began to appear at a potential negative to −3.3 V, accompanying intense hydrogen gas bubbles, and the formation rate became faster while the applied potential was negatively shifted further. A current of −5 V was chosen here to obtain enough Sb NPs quickly in 200 s. The electrode surface of Sb also became rough after the cathodic dispersion in 4 M NaOH for 200 s, which was shown in Fig. 6b. The dissolved length of the electrode by the dispersion was ca. 70 μm and the lost metal (ca. 2 mg) from the Sb electrode was mostly transferred into Sb colloid (Fig. 6a, inset) in the catholyte, except for a small amount of escaped SbH_3. We will discuss this fact in Scheme 2 in Proposed mechanisms on the formation of Sb NPs via the cathodic dispersion with different media.

A typical TEM image of Sb NPs prepared in 4 M NaOH is shown in Fig. 7A. It can be seen that the average size of Sb NPs is about 30 nm. However, there are some larger ones ca. 50 nm and smaller ones ca. 20 nm. The representative XRD patterns of Sb NPs collected from the NaOH solution are demonstrated in Fig. 7B. The diffraction peaks of the Sb NPs can be indexed to hexagonal Sb (JCPDS 85–1323). The two strong peaks of Raman spectrum in Fig. 7C(a) at 114 and 147 cm^{-1} for the NPs prepared in 4 M NaOH are also characteristic for antimony [1, 19, 20]. There is only one weak peak at 251 cm^{-1} for Sb_2O_3 [1, 21], which indicates that the oxide shell was too thin to be detected by Raman, not to mention XRD.

A more sensitive technique, XPS, was adopted to identify the surface chemical state and composition of the Sb NPs prepared in 4 M NaOH. As shown in Fig. 7D, the Sb $3d_{3/2}$ and Sb $3d_{5/2}$ peaks clearly show two antimony environments: Sb^{3+} at 539.72 and 530.30 eV and Sb^0 at 537.03 and 527.63 eV corresponding to Sb_2O_3 and metallic antimony, respectively. These assignments are in good agreement with results previously reported in the literature [1, 21–24]. The atomic ratio of Sb(0)/Sb(III) at the surface of the Sb NPs is 3.14% : 96.86%. Additionally, two O 1s signals were obtained at 531.1 and 532.9 eV. The O 1s peak denoted as c_1 is assigned to the oxygen element in

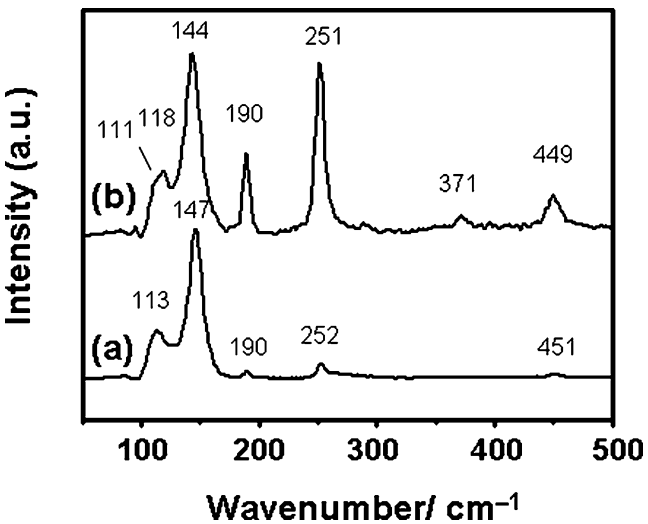

Fig. 5 Raman spectra of Sb NPs prepared in 0.1 M TBAB acetonitrile solution **a** before and **b** after heating to 225 °C for 15 min under Ar atmosphere

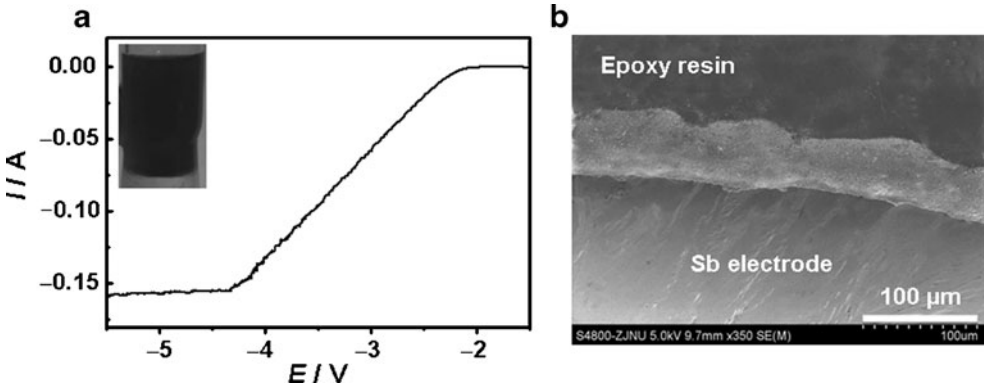

Fig. 6 **a** Linear scan voltammogram at 100 mV/s for the polished bulk Sb electrode (2.5 mm diameter) in 4 M NaOH. *Inset*: Sb colloid from the cathodic dispersion of the Sb electrode in 4 M NaOH. **b** SEM image of Sb electrode after cathodic dispersion in 4 M NaOH for 200 s

Sb_2O_3, while the O 1s peak denoted as c_2 came from other sources like hydroxyl or other adsorbed oxygen-containing species during synthesis and/or post-exposure in air [24]. These XPS spectra clearly show that the surface of Sb NPs is covered by an ultrathin layer of Sb_2O_3 and adsorbed oxygen-containing species.

By the analyses of the above XPS, XRD and Raman data, we can conclude that Sb NPs prepared in NaOH solution are not so easily oxidized by oxygen in the air, comparing with the Sb NPs prepared in acetonitrile solution. Thus no additional organic protective agents are required in the solution of NaOH in view of that the strong adsorption of hydroxide ions from the solution could stabilize the Sb NPs. Since Sb NPs prepared in acetonitrile solutions and in aqueous NaOH solutions were amorphous and hexagonal, respectively, that might be one reason for

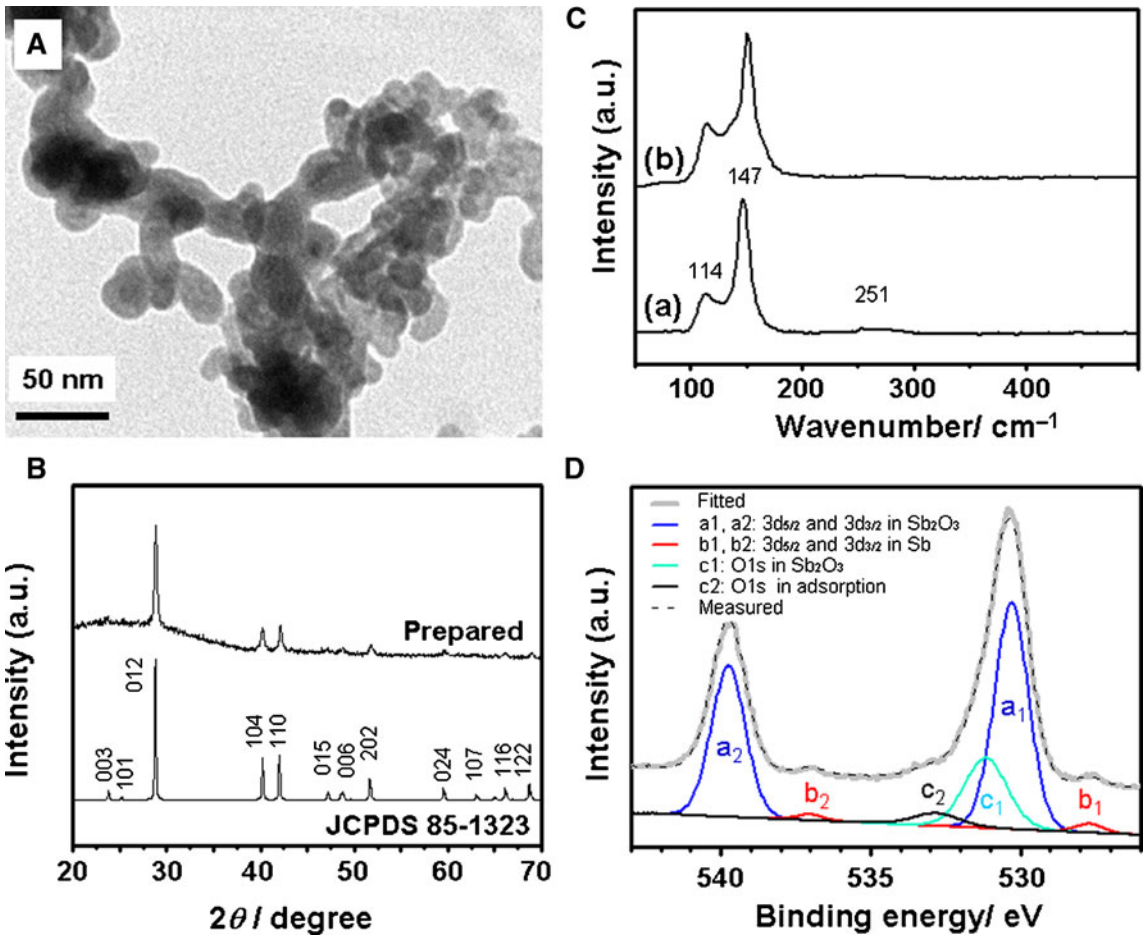

Fig. 7 Characterizations of Sb NPs prepared in 4 M NaOH by **A** TEM, **B** XRD, **C** Raman spectroscopy, and **D** high-resolution XPS. The *measured* and *fitted lines* in (D) have the same offset for clarity. The Raman spectrum of (b) in (C) is for the sample from the decomposition of volatile SbH_3 on the solid NaOH

the difference in color for the two colloids prepared in different media. Another reason might be their difference in size, which can be seen in their TEM images.

Proposed mechanisms on the formation of Sb NPs via the cathodic dispersion with different media

A mechanism proposed for the formation of Sb NPs via cathodic dispersion of Sb electrodes in TBAB acetonitrile solutions is given in Scheme 1:

$$Sb + (C_4H_9)_4N^+ + e^- \rightarrow (C_4H_9)_4N^+Sb_5^- \xrightarrow{\text{alcohol}} SbNPs + H_2 \quad (1)$$

At sufficient negative potentials, a Zintl compound $(C_4H_9)_4N^+Sb_5^-$ can be formed as a result of reaction between tetrabutylammonium cations (TBA^+) and negatively charged Sb electrode. Many Zintl ion salts including Bi, Hg, Pb, Sb and Sn have been investigated during the cathodic polarization [25–27]. These Zintl salts are strong reducing agents and were usually used in organic syntheses [28–30]. In our case, the in situ electrogenerated Zintl compound $(C_4H_9)_4N^+Sb_5^-$ can be easily oxidized by the proton from the added protic solvent, alcohol, yielding Sb NPs and hydrogen continuously. Our work is a combination of those two portions in the literature and our purpose is to disperse bulk Sb electrodes into Sb NPs.

The situation in NaOH solutions seems more complicated for the cathodic dispersion of Sb electrodes into Sb NPs. We have studied the cathodic dispersion of bulk Sb under a series of concentrations of NaOH ranging from 0.1 to 8 M. We found that Sb cathodes could not be dispersed below 1 M NaOH even the applied potential was negative to −4.0 V. The Sb cathode began to disperse slowly when the applied potential was negative to −3.7 V in 2 M NaOH. However, cathodic dispersion of Sb electrodes proceeded easily in 8 M NaOH as long as the applied potential was negative to −3.0 V. These facts demonstrate that the cathodic dispersion of bulk Sb in NaOH solution is closely related to the concentration of NaOH and the applied potential. A mechanism proposed for the cathodic dispersion of Sb electrodes in NaOH solutions is given in Scheme 2:

$$\begin{array}{l} Sb + nNa^+ + e^- \rightarrow Na_nSb \xrightarrow{H_2O} Sb\ NPs \\ \qquad\qquad \downarrow e^- \\ \qquad\qquad Sb_7^{3-} \xrightarrow{H_2O} Sb\ NPs \\ \qquad\qquad \downarrow H_2O \\ Sb + 3H^+ + 3e^- \rightarrow SbH_3 \xrightarrow{\text{decomposition}} SbNPs \end{array} \quad (2)$$

Under highly cathodic polarization negative to −5 V, Na^+ ions can be reduced to Na [31] and incorporated into the Sb cathode forming intermetallic compound Na_nSb [32–34]. The intermetallic compound formed on the cathode surface reacted with water [34], thereby transforming into Sb NPs. According to Gladyshev [32], intermetallic compound under strong cathodic polarization can be transformed into polyanions Sb_7^{3-} (Zintl ions). The polyanions Sb_7^{3-} are very unstable in water, and they can react with the surrounding water molecules, leading to cathodic dispersion, hydrogen evolution and formation of hydrides (SbH_3) [32]. SbH_3 is also very unstable in alkaline solution [14, 35] and can decompose to metal Sb. However, a small portion of the produced SbH_3 was able to escape from the solution, and we absorbed it with solid NaOH since SbH_3 is a kind of very poisonous gas. We observed that the surface of solid NaOH turned to black when cathodic dispersion took place. The black substance was metal Sb characterized by Raman spectroscopy as shown in Fig. 4C(b). Another way to produce SbH_3 is by direct formation due to the reduction of water molecules on the cathode surface [36, 37]. Thus, the incorporation of Na, the formation/oxidation of Sb polyanions and the formation/decomposition of volatile unstable antimony hydrides may all have an impact on the cathodic dispersion of bulk Sb electrodes in aqueous NaOH solutions. However, no SbH_3 can be detected during the dispersion of Sb electrodes in TBAB acetonitrile solutions.

By comparing the dispersion of Sb electrodes in the TBAB acetonitrile solution and in the NaOH solution under highly cathodic polarization, it is reasonable to believe that the formation/oxidation of polyanions Sb_n^{x-} may be a necessary step in these two cathodic dispersion processes because no antimony hydride was involved in the acetonitrile solution.

Conclusions

To conclude, Sb NPs have been prepared by dispersing a bulk antimony electrode under highly cathodic polarization both in TBAB acetonitrile solution and in aqueous NaOH solution at room temperature. The as-prepared Sb NPs in the acetonitrile solution is easily oxidized by oxygen in the air during post treatment and characterization, forming Sb–Sb_2O_3 core–shell NPs. While the Sb NPs are being prepared in the NaOH solution, they are inert to oxygen in the air due to the protection provided by strongly adsorbed hydroxide ions from the solution. Zintl ions Sb_n^{x-} seem to be involved in the cathodic dispersion processes both in the TBAB acetonitrlie solution and in the alkaline solution.

Acknowledgements We are grateful for the financial support provided by the Natural Science Foundation of Zhejiang Province of China (Grant No. Y4090658), the Open Foundation of Key Laboratory of the Ministry of Education for Advanced Catalysis Materials and Zhejiang Key Laboratory for Reactive Chemistry on Solid Surfaces (Grant No. DH201001), PhD Programs Foundation of the Education Ministry of China (Grant No. 20104306110003) and National Natural Science Foundation of China (Grant Nos. 20673103 and 21003045).

References

1. Bryngelsson H, Eskhult J, Nyholm L, Herranen M, Alm O (2007) Electrodeposited Sb and Sb/Sb_2O_3 nanoparticle coating as anode materials for Li-ion batteries. Chem Mater 19:1170
2. Kim H, Cho J (2008) Template synthesis of hollow Sb nanoparticles as a high-performance lithium battery anode material. Chem Mater 20:1679
3. Simonin L, Lafont U, Tabrizi N, Schmidt-Ott A, Kelder EM (2007) Sb/O nano-composites produced via spark discharge generation for Li-ion battery anodes. J Power Sources 174:805
4. Hočevar SB, Švancara I, Ogorevc B, Vytřas K (2007) Antimony film electrode for electrochemical stripping analysis. Anal Chem 79:8639
5. Urbanová V, Vytřas K, Kuhn A (2010) Macroporous antimony film electrodes for stripping analysis of trace heavy metals. Electrochem Chem 12:114
6. Barati M, Chow JCL, Ummat PK, Datars WR (2001) Temperature dependence of the resistance of antimony nanowire arrays. J Phys Condens Matter 13:2955
7. Wang YM, Hong BH, Lee JY, Kim JS, Kim GH, Kim KS (2004) Antimony nanowires self-assembled from Sb nanoparticles. J Phys Chem B 108:16723
8. Zhou B, Hong JM, Zhu JJ (2005) Microwave-assisted rapid synthesis of antimony dendrites. Mater Lett 59:3081
9. Warren SC, Jackson AC, Cater-Cyker ZD, DiSalvo FJ, Wiesner U (2007) Nanoparticle synthesis via the photochemical polythiol process. J Am Chem Soc 129:10072
10. Huang W, Chen S, Zhen JF, Li ZL (2009) Facile preparation of Pt hydrosols by dispersing bulk Pt with potential perturbations. Electrochem Commun 11:469
11. Liu J, Huang W, Chen S, Hu S, Li ZL (2009) Facile electrochemical dispersion of bulk Rh into hydrosols. Int J Electrochem Sci 4:1302
12. Chen X, Chen S, Huang W, Zhen JF, Li ZL (2009) Facile preparation of Bi nanoparticles by novel cathodic dispersion of bulk bismuth electrodes. Elecrtochim Acta 54:7370
13. Huang W, Fu L, Yang YC, Hu S, Li C, Li ZL (2010) Simultaneous fabrications of nanoparticles and 3D porous films of Sn or Pb from pure electrodes. Electrochem Solid State Lett 13:K46
14. Grochala W, Edwards PP (2004) Thermal decomposition of the non-interstitial hydrides for the storage and production of hydrogen. Chem Rev 104:1283
15. Balan L, Dailly A, Schneider R, Billaud D, Willmann P, Olivier-Fourcade J, Jumas JC (2005) Synthesis of nanoscale antimony particles. Hyperfine Interact 165:101
16. Dailly A, Schneider R, Billaud D, Fort Y, Ghanbaja J (2003) Nanometric antimony powder synthesis by activated alkaline hydride reduction of antimony pentachloride. J Nanopart Res 5:389
17. Fuchs G, Treilleux M, Santos-Aires F, Melinon P, Cabaud B, Hoareau A (1991) Crystallization of thin antimony deposits on amorphous carbon. Thin Solid Films 204:107
18. Taft E, Apker L (1954) Fermi level in amorphous antimony films. Phys Rev 96:1496
19. Wang X, Kunc K, Loa I, Schwara UD, Syassen K (2006) Effect of pressure on the Raman modes of antimony. Phys Rev B 74:134305
20. Eberle B, Sontag H, Weber R (1985) Raman spectroscopy of matrix-isolated antimony and bismuth and bismuth clusters. Surf Sci 156:751
21. Zeng DW, Xie CS, Zhu BL, Song WL (2004) Characteristics of Sb_2O_3 nanoparticles synthesized from antimony by vapor condensation method. Mater Lett 58:312
22. Morgan WE, Setc WJ, Van Wazer JR (1973) Inner-orbital binding-energy shifts of antimony and bismuth compounds. Inorg Chem 12:953
23. Santinacci L, Sproule GI, Moisa S, Landheer D, Wu X, Banu A, Djenizian T, Schmuki P, Graham MJ (2004) Growth and characterization of thin anodic oxide films on n-InSb(100) formed in aqueous solutions. Corros Sci 46:2067
24. Pérez OEL, Sánchez MD, Teijelo MLJ (2010) Characterization of growth of anodic antimony oxide films by ellipsometry and XPS. J Electroanal Chem 645:143
25. Svetličić V, Lawin PB, Kariv-Miller E (1990) Reaction of solid cathodes with tetraalkylammonium electrolytes. J Electroanal Chem 284:185
26. Kariv-Miller E, Lawin PB, Vajtner Z (1985) The reduction of tetraalkylammonium ions on metal electrodes: Cathodic corrosion and "tetraalkylammonium-metals". J Electroanal Chem 195:435
27. Fidler MM, Svetlicic V, Kariv-Miller E (1993) An electrochemical study of antimony cathodes in tetraalkylammonium electrolyte solutions. J Electroanal Chem 360:221
28. Kariv-Miller E, Nanjundiah C, Eaton J, Swenson KE (1984) Dimethylpyrrolidinium amalgam formation and catalysis of organic electroreductions. J Electroanal Chem 167:141
29. Kariv-Miller E, Andruzzi R (1985) Dimethylpyrrolidinium, a catalyst for organic electroreductions. J Electroanal Chem 187:175
30. Kariv-Miller E, Vajtner Z (1985) Electroreductive Dehalogenation of Fluorobenzenes. J Org Chem 50:1394
31. Montes L, Lagowski JJ (2003) Electrochemical Behavior of Sodium Anions. J Phys Chem B 107:10665
32. Gladyshev VP, Zhanbyrbaeva MB (1982) Mechanism of the cathodic dispersion of p-elements. J Appl Chem USSR 55:1882
33. Kabanov BN, Astakhov II, Kiseleva IG (1979) Formation of crystalline intermetallic compounds and solid solutions in electrochemical incorporation of metals into cathodes. Electrochim Acta 24:167
34. Kabanov BN, Astakhov II, Kiseleva IG (1965) Electrochemical implantation of alkali metals. Russ Chem Rev 34:775
35. Grant J (1928) The determination of small quantities of antimony in the form of stibine. Analyst 53:626
36. Varma R, Tomczuk Z, Kazadi S, Yao NP (1989) Stibine and arsine generation from a lead-acid cell during charging modes under a utility load-leveling duty cycle. J Appl Electrochem 19:10
37. Zhang WB, Yang XA, Dong YP, Chu XF (2010) Application of alkaline mode electrochemical hydride generation for the detection of As and Sb using atomic fluorescence spectrometry. Spectrochim Acta B 65:571